IJSCE : Vol. 4 • No. 2 • July-December 2012 • pp. 115-121 © *Research Science Press*

Deflection and Stress Resultants of Composite Hypar Shell Roofs Under Point Load and Complex Boundary Conditions

Sarmila Sahoo
Department of Civil Engineering, Heritage Institute of Technology, Kolkata-700107, India
(E-mail: sarmila.sahoo@gmail.com)

Abstract: An eight noded doubly curved shell bending element is used in the present analysis having five degrees of freedom per node. The stiffness matrix is derived following the conventional method of minimization of potential energy and a lumped load vector is adopted. Benchmark problems are solved taking vibration problems of twisted plates. Numerical experiments are conducted taking six boundary conditions and eight stacking sequences of graphite epoxy composite. Results of static deflection and moment resultants are furnished and analysed to understand the relative efficiencies of two or more shell options having different boundary conditions and laminations.

Keywords: Composite hypar shell, bending behaviour, critical boundary condition, concentrated load, finite element analysis.

1. INTRODUCTION

Hyperbolic paraboloid shell bounded by straight line (commonly known as hypar shell) is a good choice as roofing unit to civil engineers. Apart from its aesthetic beauty this ruled surface is easy to fabricate and can allow entry of north light, which are preferred in medicine and food processing industries. Since the laminated composite emerged as improved structural material from the second half of the last century the civil engineers also applied these materials for fabricating plates and shells to be used as roofing units. Schwarte [1] worked on free vibration of isotropic rhombic hypar shell and the twisted plates which have structural resemblance with hypar shells received attention from several authors like Kielb [2], Seshu and Ramamurti [3] and others. Chakravorty *et al.* [4] in 1998 reported natural and forced vibration response of corner point supported skewed hypar shell.

It is evident that the study about composite hypar shell is far from complete. In a recent paper Sahoo and Chakravorty [5] have reported static shell actions of composite hypar shells under uniform loading only. Hence the present endeavour is to explore the bending characteristics of such shells under concentrated load for different practical boundary conditions.

2. MATHEMATICAL FORMULATION AND SOLUTION

An eight-noded curved quadratic isoparametric finite element is used for the formulation. The five degrees of freedom taken into consideration at each node are u, v, w, α, β. The strain-displacement relations on the basis of improved first order approximation theory for thin shell are established as

$$\{\varepsilon_x\ \varepsilon_y\ \gamma_{xy}\ \gamma_{xz}\ \gamma_{yz}\}^T = \{\varepsilon_x^0\ \varepsilon_y^0\ \gamma_{xy}^0\ \gamma_{xz}^0\ \gamma_{yz}^0\}^T + z\{k_x\ k_y\ k_{xy}\ k_{xz}\ k_{yz}\}^T \tag{1}$$

where the first vector is the mid-surface strain for a hypar shell and the second vector is the curvature. These are given, respectively, by

$$\begin{Bmatrix} \varepsilon_x^0 \\ \varepsilon_y^0 \\ \gamma_{xy}^0 \\ \gamma_{xz}^0 \\ \gamma_{yz}^0 \end{Bmatrix} = \begin{Bmatrix} \partial u/\partial x \\ \partial v/\partial y \\ \partial u/\partial y + \partial v/\partial x - 2w/R_{xy} \\ \alpha + \partial w/\partial x \\ \beta + \partial w/\partial y \end{Bmatrix},$$

$$\begin{Bmatrix} k_x \\ k_y \\ k_{xy} \\ k_{xz} \\ k_{yz} \end{Bmatrix} = \begin{Bmatrix} \partial \alpha/\partial x \\ \partial \beta/\partial y \\ \partial \alpha/\partial y + \partial \beta/\partial x \\ 0 \\ 0 \end{Bmatrix} \tag{2}$$

A laminated composite hypar shell of uniform thickness h and twist radius of curvature *Rxy* is considered. Keeping the total thickness same, the thickness may consist of any number of thin laminae each of which may be arbitrarily oriented at an angle θ with reference to the *x*-axis of the co-ordinate system. The constitutive equations for the shell are given by

$$\{F\} = [D]\{\varepsilon\} \tag{3}$$

where, $\{F\} = \{N_x\ N_y\ N_{xy}\ M_x\ M_y\ M_{xy}\ Q_x\ Q_y\}^T$,

$$[D] = \begin{bmatrix} [A] & [B] & [0] \\ [B] & [D] & [0] \\ [0] & [0] & [S] \end{bmatrix},$$

$$\{\varepsilon\} = \{\varepsilon_x^0\ \varepsilon_y^0\ \gamma_{xy}^0\ k_x\ k_y\ k_{xy}\ \gamma_{xz}^0\ \gamma_{yz}^0\}^T. \tag{4}$$

The stiffness coefficients are defined as

$$A_{ij} = \sum_{k=1}^{np} (Q_{ij})_k (z_k - z_{k-1});$$

$$B_{ij} = \frac{1}{2} \sum_{k=1}^{np} (Q_{ij})_k (z_k^2 - z_{k-1}^2);$$

$$D_{ij} = \frac{1}{3}\sum_{k=1}^{np}(Q_{ij})_k(z_k^3 - z_{k-1}^3)\ i, j = 1, 2, 6;$$

$$S_{ij} = \sum_{k=1}^{np} F_i F_j (G_{ij})_k (z_k - z_{k-1})\ i, j = 1, 2; \tag{5}$$

where *Qij* are elements of the off-axis elastic constant matrix which are derived from appropriate transformation of the on-axis matrix. *Fi* and *Fj* are shear correction factors presently taken as unity. The terms of the on-axis matrix depend on the elastic moduli and Poisson's ratio of the material. The element stiffness matrix and the load vector are derived through the routine steps of finite element formulation employing numerical integration. The element stiffness matrix and the element load vectors are assembled to get the global matrices. The basic equation of statics is solved by Gaussian elimination algorithm.

3. NUMERICAL EXAMPLES

Cantilever twisted plates are solved (done earlier by Qatu and Leissa [6]) to obtain the non-dimensional fundamental frequencies and the present results are compared with the published ones (Table 1). The authors take the liberty to use this bench mark problem due to unavailability of results of bending analysis of shells with cross curvature.

Table 1
Non-dimensional Natural Frequencies $\bar{\omega}$ [= $\omega\, a^2\, (\rho/E_{11}h^2)$] for Three Layer Graphite Epoxy Twisted Plates, [θ /-θ /θ] Laminate

	θ *(degree)*	*0*	*15*	*30*	*45*	*60*	*75*	*90*
$\phi=15^0$	Qatu and Leissa [6]	1.0035	0.9296	0.7465	0.5286	0.3545	0.2723	0.2555
	Present FEM	0.9989	0.9258	0.7443	0.5278	0.3541	0.2720	0.2551

a/b = 1, a/h = 100; E_{11} = 138 GPa, E_{22} = 8.96 GPa, G_{12}= 7.1 GPa, ν_{12} = 0.3.

Additional problems of skewed hypar shells are also solved. The different stacking sequences taken are antisymmetric cross ply ($0^0/90^0$ – ASCP), symmetric cross ply ($0^0/90^0/0^0$ – SYCP), antisymmetric angle ply ($45^0/-45^0$ – ASAP) and symmetric angle ply ($45^0/-45^0/45^0$ – SYAP) laminates. The different boundary conditions are as shown in Figure 1. The results of transverse deflection and various force and moment resultants are obtained but for the sake of brevity only deflection and some moment resultants are presented in the form of tables using the non-dimensional parameters $\bar{w}$, $\bar{M}_x$, $\bar{M}_y$. In all the cases only the converged results are presented in Tables 2-4. A particular shell action is taken to have converged for particular finite element grid, if further refinement of the grid does not improve that result by more than one per cent. With this criterion an 8x8 mesh is found to be appropriate for all the problems taken up here.

4. RESULTS AND DISCUSSIONS

From Table 1 it is found that the fundamental frequencies of cantilever twisted plates obtained by Qatu and Leissa [6] using a laminated shallow shell theory compare well with the present results. So the correctness of the present approach incorporating the effect of twist of curvature in the formulation is established.

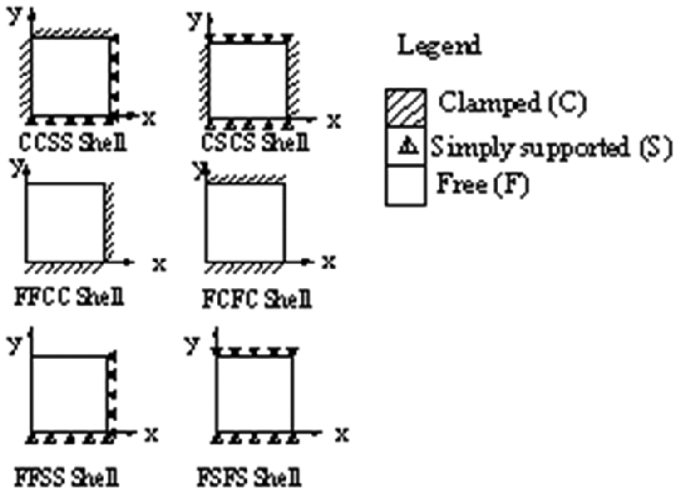

Figure 1: Arrangement of Boundary Conditions

4.1. Effect of Number of Boundary Constraints on Static Deflection

Group III shells have the least number of boundary constraints followed by Group II ones and then finally by Group I ones. As expected Group I shells show less deflection than Group II ones which in turn exhibit lesser deflections than Group III shells as seen in Table-2. This is expected that introduction of support restraints makes a shell stiffer, although increased number of boundary restraints may increase other shell actions. It is noted that for cross-ply ($0^0/90^0$, $0^0/90^0/0^0$) shells when a Group II boundary is changed to a Group III one, the relative increase in deflection is very significant compared to the case when a Group I edge in turn is changed to a Group II condition. But for angle ply ($+45^0/-45^0$, $+45^0/-45^0/+45^0$) shells the change in deflection due to change in boundary constraints is quite significant in all the cases.

Table 2
Values of Maximum Non-dimensional Downward Deflection ($\bar{w}$) x10^4 for Different Laminations and Boundary Conditions where ($\bar{x}$, $\bar{y}$) is the Location of Maximum Deflection

Lamination (degree)	*Boundary conditions*					
	Group I		*Group II*		*Group III*	
	A	*B*	*A*	*B*	*A*	*B*
	CCSS	*CSCS*	*FFCC*	*FCFC*	*FFSS*	*FSFS*
0/90	-23.959	-27.706	-24.163	-29.554	-51.351	-43.595
	(0.5, 0.5)	(0.5, 0.5)	(0.5, 0.5)	(0.5, 0.5)	(0.5, 0.5)	(0.5, 0.5)
0/90/0	-21.272	-30.561	-21.647	-21.282	-47.134	-36.015
	(0.5, 0.5)	(0.5, 0.5)	(0.5, 0.5)	(0.5, 0.5)	(0.5, 0.5)	(0.5, 0.5)
45/-45	-19.456	-19.826	-25.817	-29.741	-35.304	-38.499
	(0.5, 0.5)	(0.5, 0.5)	(0.5, 0.5)	(0.5, 0.5)	(0.5, 0.5)	(0.5, 0.5)
45/-45 /45	-14.102	-14.138	-18.048	-18.603	-24.828	-24.561
	(0.5, 0.5)	(0.5, 0.5)	(0.5, 0.5)	(0.5, 0.5)	(0.5, 0.5)	(0.5, 0.5)

$a/b = 1$, $a/h = 100$, $c/a = 0.2$; $E_{11} = 25E_{22}$, $G_{12} = G_{13} = 0.5E_{22}$, $G_{23} = 0.2\ E_{22}$, $\nu_{12} = \nu_{21} = 0.25$

Table 3

Values of Numerically Maximum Non-dimensional Moment $\bar{M}_x$ [$=M_x/qa^2$] x10^2 for Different Laminations and Boundary Conditions where ($\bar{x}$, $\bar{y}$) is the Location of Maximum Moment in Each Case

Lamination (degree)	Boundary conditions: Group I A	Group I B	Group II A	Group II B	Group III A	Group III B
	CCSS	*CSCS*	*FFCC*	*FCFC*	*FFSS*	*FSFS*
0/90	-17.212	-18.541	-17.244	-16.972	-19.505	-19.006
	(0.5, 0.5)	(0.5, 0.5)	(0.5, 0.5)	(0.5, 0.5)	(0.5, 0.5)	(0.5, 0.5)
0/90/0	-9.0661	-10.232	-9.0978	-8.8419	-10.980	-10.381
	(0.5, 0.5)	(0.5, 0.5)	(0.5, 0.5)	(0.5, 0.5)	(0.5, 0.5)	(0.5, 0.5)
45/-45	-12.047	-12.199	-12.950	-13.500	-13.682	-14.275
	(0.5, 0.5)	(0.5, 0.5)	(0.5, 0.5)	(0.5, 0.5)	(0.5, 0.5)	(0.5, 0.5)
45/-45 /45	-21.036	-21.139	-22.508	-22.614	-24.052	-24.025
	(0.5, 0.5)	(0.5, 0.5)	(0.5, 0.5)	(0.5, 0.5)	(0.5, 0.5)	(0.5, 0.5)

$a/b = 1$, $a/h = 100$, $c/a = 0.2$; $E_{11} = 25E_{22}$, $G_{12} = G_{13} = 0.5E_{22}$, $G_{23} = 0.2E_{22}$, $\nu_{12} = \nu_{21} = 0.25$

4.2. Effect of Stacking Sequences on Static Deflection

For shells of Group I and Group III boundaries condition angle ply laminates prove their prominent superiority over the cross ply ones. For Group II boundary any one among angle ply and cross ply stacking orders may be chosen. Apart from symmetric cross ply shells with CSCS edge condition for all other cases symmetric laminates are better choices than anti-symmetric ones from deflection criterion. The effect of stacking sequence on moment resultants is rather complicated and to correctly estimate the behaviour a detailed analysis is necessary.

Table 4

Values of Numerically Maximum Non-dimensional Moment $\bar{M}_y$ [$= M_y/qa^2$] x10^2 for Different Laminations and Boundary Conditions ($\bar{x}$, $\bar{y}$) is the Location of Maximum Moment in Each Case

Lamination (degree)	Boundary conditions: Group I A	Group I B	Group II A	Group II B	Group III A	Group III B
	CCSS	*CSCS*	*FFCC*	*FCFC*	*FFSS*	*FSFS*
0/90	-17.261	-16.929	-17.308	-19.180	-19.732	-19.681
	(0.5, 0.5)	(0.5, 0.5)	(0.5, 0.5)	(0.5, 0.5)	(0.5, 0.5)	(0.5, 0.5)
0/90/0	-34.739	-34.290	-34.901	-35.796	-38.688	-36.103
	(0.5, 0.5)	(0.5, 0.5)	(0.5, 0.5)	(0.5, 0.5)	(0.5, 0.5)	(0.5, 0.5)
45/-45	-12.051	-12.091	-12.951	-14.240	-13.712	-15.155
	(0.5, 0.5)	(0.5, 0.5)	(0.5, 0.5)	(0.5, 0.5)	(0.5, 0.5)	(0.5, 0.5)
45/-45 /45	-21.039	-21.054	-22.521	-22.983	-24.087	-24.387
	(0.5, 0.5)	(0.5, 0.5)	(0.5, 0.5)	(0.5, 0.5)	(0.5, 0.5)	(0.5, 0.5)

$a/b = 1$, $a/h = 100$, $c/a = 0.2$; $E_{11} = 25E_{22}$, $G_{12} = G_{13} = 0.5E_{22}$, $G_{23} = 0.2E_{22}$, $\nu_{12} = \nu_{21} = 0.25$

Table 5
Materials Arranged According to Ascending Order of Magnitudes of Shell Actions

Non-dimensional shell actions	*Non-dimensional Co-ordinates* $(\bar{x},\bar{y})$	*Materials in ascending order*
	(0.5, 0.5)	CCSS/SYAP
	(0.5, 0.5)	CSCS/SYAP
$\bar{w}$	(0.5, 0.5)	FFCC/SYAP
	(0.5, 0.5)	FCFC/SYAP
	(0.5, 0.5)	FSFS/SYAP
	(0.5, 0.5)	FFSS/SYAP
	(0.5, 0.5)	FCFC/SYCP
	(0.5, 0.5)	CCSS/SYCP
$\bar{M}_x$	(0.5, 0.5)	FFCC/SYCP
	(0.5, 0.5)	CSCS/SYCP
	(0.5, 0.5)	FSFS/SYCP
	(0.5, 0.5)	FFSS/SYCP
	(0.5, 0.5)	CCSS/ASAP
	(0.5, 0.5)	CSCS/ASAP
$\bar{M}_y$	(0.5, 0.5)	FFCC/ASAP
	(0.5, 0.5)	FFSS/ASAP
	(0.5, 0.5)	FCFC/ASAP
	(0.5, 0.5)	FSFS/ASAP

4.2.1. Performances of Different Boundary Conditions with Respect to Different Shell Actions

Corresponding to each shell action (deflection and bending moments presented in Tables 2-4) the best two combinations of lamination and edge condition are selected from each boundary condition. These six combinations obtained from three groups of boundary conditions are furnished in Table 5 in ascending order of magnitude. In the present analysis upward deflection and hogging moments are considered positive. However, the values of positive (upward) deflections are left out from the tables because those are found to be negligible compared to downward deflections. This rank wise arrangement of the shells corresponding to the different shell actions will be helpful to a practicing engineer because, if he knows that which shell action is critical for a particular situation, he can make a choice among a number of options. It is interesting to note that the superiority of a particular combination of lamination and boundary condition in terms of deflection over another combination cannot form the basis of predicting their relative performances in terms of moment resultants.

From results of Table 5 it is very interesting to note that corresponding to $\bar{w}$, $\bar{M}_x$ and $\bar{M}_y$, SYAP, SYCP and ASAP shells perform better respectively and for each of the shell actions only one lamination turn out to be the best choice whatever be the boundary condition. Since anti-symmetric cross-ply laminate does not figure as the best choice in any of the cases it may be considered to be relatively inferior option among the four laminates considered here.

The relative performances of different boundary options may be studied by comparing sum of their ranks (among 6) corresponding to $\bar{w}$, $\bar{M}_x$ and $\bar{M}_y$ from Table 5. Between any two boundary conditions the one securing the less sum of ranks may be considered as the better option. In this line the sum of the ranks for CCSS boundary is least (= 4) and hence may be regarded as the best boundary conditions. The corresponding value of CSCS, FFCC and FCFC edges are eight, nine and ten respectively and these edges may be described as having comparable performances.

5. CONCLUSIONS

The following conclusions are drawn from the present study:

1. The finite element model proposed here can successfully analyze bending problems of skewed hypar shells, which is reflected by close agreement of present results with benchmark one.

2. An increase in the number of support constraints always reduces the deflection but may increase other shell actions. Hence for a complete knowledge about all shell actions, a detailed study is needed.

3. Of the different lamination considered here performance of ASCP is poor and that of the other three are comparable both in terms of deflection and moment resultants.

4. Among the different boundary conditions under present consideration CCSS turns out to be the best followed by CSCS, FFCC and FCFC edges, which show comparable performance. FFSS and FSFS boundaries show poor performance. This conclusion considers both deflection and moment resultants.

References

[1] J. Schwarte (1994), “Vibrations of Corner Point Supported Rhombic Hypar-shells”, *J. Sound Vibr.,* 175 (1), pp. 105-114.

[2] R. E. Kielb, A. W. Leissa and J. C. Macbain (1985), “Vibrations of Twisted Cantilever Plates - A Comparison of Theoretical Results”. *Int. J. for Num. Methods in Engng.,* 21, pp. 1365-1380.

[3] P. Seshu and V. Ramamurti (1989), “Vibrations of Twisted Composite Plates”. *J. Aeronautical Soc. India,* 41, pp. 65-70.

[4] D. Chakravorty, J. N. Bandyopadhyay and P. K. Sinha (1998), “Applications of FEM on Free and Forced Vibrations of Laminated Shells”. *ASCE, J. Engng. Mech.,* 124 (1), pp. 1-8.

[5] S. Sahoo and D. Chakravorty (2004), “Finite Element Bending Behaviour of Composite Hyperbolic Paraboloidal Shells with Various Edge Conditions”. *J. Strain Analysis for Engng. Design,* 39 (5), pp. 499-513.

[6] M. S. Qatu and A. W. Leissa (1991), “Vibration Studies for Laminated Composite Twisted Cantilever Plates”, *Int. J. Mech. Sc.,* 33 (11), pp. 927-940.